Lyapunov Stability of a Nonlinear Bio-inspired System for the Control of Humanoid Balance

Vittorio Lippi[a] and Fabio Molinari[b]

Technische Universität Berlin, Fachgebiet Regelungssysteme, Einsteinufer 17 D-10587, Berlin, Germany

Keywords: Posture Control, Humanoid, Stability.

Abstract: Human posture control models are used to analyse neurological experiments and control of humanoid robots. This work focuses on a well-known nonlinear posture control model, the DEC (Disturbance estimate and Compensation). In order to compensate disturbances, unlike other models, DEC feedbacks signals coming from sensor fusion rather than *raw* sensory signals. In previous works, the DEC model is shown to predict human behavior and to provide a control system for humanoids. In this work, the stability of the system in the sense of Lyapunov is formally analysed. The theoretical findings are combined with simulation results, in which an external perturbation of the support surface reproduces a typical scenario in posture control experiments.

1 INTRODUCTION

Mathematical models of human balance are used for the analysis of neurological experiments (van der Kooij et al., 2007; van der Kooij et al., 2005; van Asseldonk et al., 2006; Goodworth and Peterka, 2018; Mergner, 2010; Engelhart et al., 2014; Pasma et al., 2014; Jeka et al., 2010; Boonstra et al., 2014), and for the control of humanoid robots. Most of human posture control studies exploit linear models such as the *independent channel* model (Peterka, 2002), that assumes a linear and time invariant behaviour (Engelhart et al., 2016). Linear models have the advantage of being simple to analyse and relatively easy to be fit on data. However, experiments reveal that human posture control exhibits important non-linearities.

In this work, we study the stability of a non-linear bio-inspired posture control system, the DEC, *Disturbance estimate and Compensation* (Mergner, 2010). The DEC model consists of a servo control loop and a compensation of external disturbances estimated on the basis of sensory inputs. The control principle can be addressed as "feed forward disturbance correction" (Luecke and McGuire, 1968; Roffel and Betlem, 2007; Zhong et al., 2012) or, in German, "Störgrößenaufschaltung" (Bleisteiner and Mangoldt, 2013). Throughout this paper, the DEC is used to model a scenario where the subject stands on a tilting surface. We analyse the effect of a dead-band nonlinearity that affects the sensory-based estimate of the support surface tilt. Such nonlinearity, common in literature, is assumed on the basis of the behaviour observed in humans. The formal conditions for Lyapunov stability are investigated.

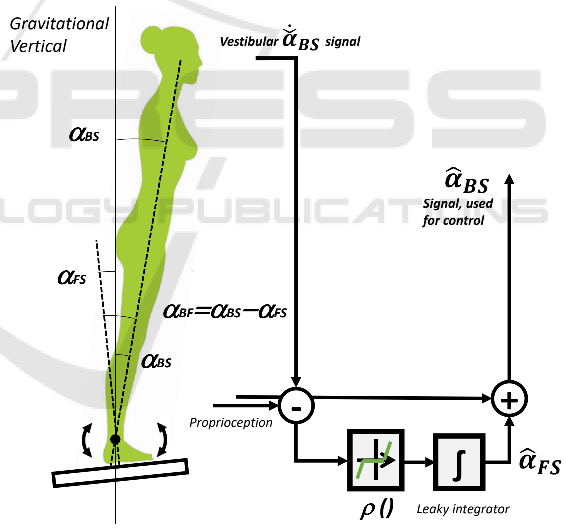

Figure 1: Posture control model. On the left: illustration of the scenario and definition of angles used in text. On the right: schema of the bio-inspired sensor fusion.

The paper is organized as follows: in Section 2, the control problem is introduced and the body mechanics is described; Section 3 provides details about human-inspired sensor fusion and actuation; the conditions

[a] https://orcid.org/0000-0001-5520-8974
[b] https://orcid.org/0000-0003-2617-962X

Lippi, V. and Molinari, F.
Lyapunov Stability of a Nonlinear Bio-inspired System for the Control of Humanoid Balance.
DOI: 10.5220/0009970307260733
In *Proceedings of the 17th International Conference on Informatics in Control, Automation and Robotics (ICINCO 2020)*, pages 726-733
ISBN: 978-989-758-442-8

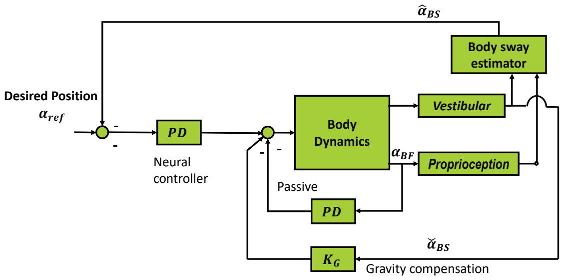

Figure 2: A scheme of a controller based on the DEC concept. The sensory inputs are used to reconstruct the physical disturbances acting on the body (in this scenario gravity and support surface tilt). The system is controlled by a servo controller, consisting of a PD regulator setting the desired body position, and a direct compensation of the estimated gravity disturbance.

for stability are obtained in Section 4, where evidence is also provided; Section 5 presents simulations and a qualitative discussion of the system behaviour; conclusions and future work are presented in Section 6.

2 PROBLEM DESCRIPTION

Human posture dynamics in the sagittal plane is usually modelled as an inverted pendulum. Depending on the scenario, the model can be a single inverted pendulum (SIP), see, e.g., (Mergner et al., 2003; Jafari et al., 2019), or a multiple inverted pendulum, see, e.g., (Alexandrov et al., 2017; Hettich et al., 2013; Lippi et al., 2013; Lippi and Mergner, 2017; Abedi and Shoushtari, 2012). The number of degrees of freedom (DoF) representing the body dynamics is in general linked to the intensity of external stimuli, see (Atkeson and Stephens, 2007) for further details. In this work, we consider a SIP model that is used to represent the upright stance in presence of small disturbances. In literature, models with 2 DoF have been used for modelling balance in the frontal plane (Goodworth and Peterka, 2010; Lippi et al., 2016).

In the remainder of this paper, we consider the following scenario: the subject is balancing on a *tilting platform* whose inclination is controlled by an external input. In order to keep the equilibrium despite the tilting movement, the orientation in space of the inverted pendulum is actively controlled by an ankle movement.

Formally, $\alpha_{BS} \in \mathbb{R}$ denotes the angle between the body (pendulum axis) and the vertical (gravity axis). $\alpha_{BF} \in \mathbb{R}$ denotes the angle between the body and the axis normal to the tilting platform. The third considered angle is $\alpha_{FS} \in \mathbb{R}$ that represents the angle of the tilting platform with regards to the vertical axis. From Figure 1, this three angles are linearly dependent, i.e.,

$$\alpha_{BF} = \alpha_{BS} - \alpha_{FS}. \tag{1}$$

The torque provided by the ankle is $T_a \in \mathbb{R}$, whereas the one produced by the gravitational force is $T_G \in \mathbb{R}$.

The pendulum dynamics is described by

$$\ddot{\alpha}_{BS} = \frac{T_a + T_p + T_G}{J_B}, \tag{2}$$

where $J_B \in \mathbb{R}_{>0}$ is the moment of inertia of the body around the ankle joint and $T_p \in \mathbb{R}$ is the torque describing passive stiffness and damping, i.e.,

$$T_p = K_p^p \alpha_{BF} + K_d^p \dot{\alpha}_{BF} \tag{3}$$

The passive stiffness, i..e, K_p^p, and damping, i.e., K_d^p, causes additional destabilisation. However, as in (Ott et al., 2016), they have a role in stabilising the system dynamics in presence of delays.

3 HUMAN-INSPIRED SENSORS AND ACTUATION

3.1 Sensors' Information

Signal $\breve{\alpha}_{BS} \in \mathbb{R}$ provides the estimate of α_{BS} (body sway) obtained by the vestibular system (or, for humanoids, by the IMU). On the other hand, signal $\breve{\alpha}_{BF} \in \mathbb{R}$ is the proprioceptive input measured at the ankle (for humanoids, given by an encoder). Both signals are estimates of the corresponding physical quantities. Their derivatives with respect to time are $\dot{\breve{\alpha}}_{BS} \in \mathbb{R}$, sensed by the vestibular system, and $\dot{\breve{\alpha}}_{BF} \in \mathbb{R}$, sensed by the proprioceptive system.

In what follows, we put a check symbol above all measured variables (i.e., $\breve{x}$). On the other hand, all estimated variables have the "hat" symbol above them (i.e., $\hat{x}$).

3.2 Gravity Compensation

The gravity force is the largest effect acting on the body, see (Zebenay et al., 2015). Formally, the torque produced by this force is

$$T_G = m_B \cdot g \cdot h_B \cdot \sin(\alpha_{BS}),$$

where g is the gravity acceleration, $m_B \in \mathbb{R}_{>0}$ the body mass, and $h_B \in \mathbb{R}_{>0}$ the height of the centre of mass. Under the assumption of a small angle,

$$T_G \simeq m_B \cdot g \cdot h_B \cdot \alpha_{BS}. \tag{4}$$

The ankle torque, actively produced by the subject in order to keep the body standing despite the tilting platform, i.e., T_a in (2), also compensates for this gravity

Table 1: List of variables and their definition. The second column contains equation numbers, in parentheses, or section number depending on where the variable is defined.

Variable	Defined in	Definition
α_{BF}	(1)	Ankle joint angle
α_{BS}	(2)	Body sway respect to the vertical
α_{FS}	§2	Support surface rotation
$\hat{\alpha}_{FS}$	(8)	Support surface rotation estimate based on sensor fusion (vestibular+proprioceptive)
$\hat{\alpha}_{BS}$	(10)	Body sway estimate based on sensory input (vestibular+proprioceptive)
$\check{\alpha}_{BS}$	§3.1	Body sway estimate based on vestibular input

disturbance. In fact, let T_a^G be the component of T_a compensating gravity, such that

$$T_a = -T_a^G + T_a^a, \tag{5}$$

where T_a^a is the ankle torque's component not due to gravity compensation. Gravity is slightly under-compensated in humans, see, e.g., (Mergner et al., 2009; Hettich et al., 2014), thus, as in (Ott et al., 2016), we assume an arbitrary gain, i.e., $K_G \in \mathbb{R}_{>0}$, for gravity compensation. Thus,

$$T_a^G = K_G \cdot \check{\alpha}_{BS}. \tag{6}$$

3.3 Support Surface Tilt Compensation

In order to reproduce the behaviour observed in humans, see, e.g., (Mergner et al., 2009; Mergner et al., 2003; Hettich et al., 2015; Hettich et al., 2014), the control input T_a^a is not computed by directly using the measured quantity $\check{\alpha}_{BS}$, but an estimate of α_{BS}, say $\hat{\alpha}_{BS}$. To this end, first, the inspection of human behaviour suggests to use signal $\dot{\check{\alpha}}_{FS} \in \mathbb{R}$, obtained by using both vestibular and proprioceptive sensed values, to estimate the tilting platform's angle. Denote this estimate by $\hat{\alpha}_{FS} \in \mathbb{R}$. This value is then used for computing $\hat{\alpha}_{BS}$, which closes the control loop.
Formally, by (1), one has

$$\dot{\check{\alpha}}_{FS} = \dot{\check{\alpha}}_{BS} - \dot{\check{\alpha}}_{BF}. \tag{7}$$

The estimate of $\hat{\alpha}_{FS}$ simulates the human behaviour. This is done by feeding $\dot{\check{\alpha}}_{FS}$ into function $\rho(\cdot)$, which is then integrated through a leaky integrator, i.e.,

$$\hat{\alpha}_{FS} = \int_0^t \rho\left(\dot{\check{\alpha}}_{FS}\right) - c_L \hat{\alpha}_{FS} d\tau \tag{8}$$

with $c_L \in \mathbb{R}_{>0}$ and the threshold function defined as

$$\rho(\alpha) := \begin{cases} \alpha + \theta & \text{if } \alpha \le -\theta \\ 0 & \text{if } -\theta < \alpha < \theta \\ \alpha - \theta & \text{if } \theta \le \alpha \end{cases}, \tag{9}$$

for $\theta \in \mathbb{R}_{>0}$.
With this piece of information at hand, we compute $\hat{\alpha}_{BS}$, the quantity used in T_a^a, by employing (1), i.e.,

$$\hat{\alpha}_{BS} = \hat{\alpha}_{FS} + \check{\alpha}_{BF}. \tag{10}$$

3.4 Other Disturbances

In order to completely describe the effect of the environment on the body, other disturbances should also be taken into account. Field forces can be produced, for example, by an horizontal translation of the support surface x_{fs} leading to a torque $T_{trans} = \ddot{x}_{fs} \cdot h_B \cdot m_B$ and an external touch that can be estimated as $T_{ext} = \ddot{\check{\alpha}}_{BS} J_B - T_a$. A robotic control applying also these disturbances is described in (Zebenay et al., 2015). Currently, a model of human support surface translation compensation is still object of research, and there are no evidences yet of a direct compensation of such disturbances. In this work only gravity will be considered.

3.5 Servo Control

As in (Ott et al., 2016), the system is controlled through a *PD* controller with proportional coefficient, respectively derivative coefficient, being $K_p^a \in \mathbb{R}$, respectively $K_d^a \in \mathbb{R}$, i.e.,

$$T_a^a = K_p^a \varepsilon + K_d^a \frac{d\varepsilon}{dt}, \tag{11}$$

where the error variable ε is defined as

$$\varepsilon := \hat{\alpha}_{BS} - \alpha_{\mathrm{ref}}, \tag{12}$$

with the desired position being, in general, $\alpha_{\mathrm{ref}} = 0$. All delays involved into the processing of sensory inputs and the motor control are not considered in this analysis. In neurology the concept was proposed in (Merton, 1953) to explain the role of the muscle stretch reflex for the control of posture and movements: a PD-controller adjusts the force of the muscles so as to produce the desired pose or movement.

Remark 1. *Gravity is compensated by directly using the available measure $\check{\alpha}_{BS}$, whilst T_a^a uses the estimated value $\hat{\alpha}_{BS}$. This is due to the fact that the non-linearity has been experimentally observed only on the latter (Mergner et al., 2009; Mergner et al., 2003; Hettich et al., 2014). Qualitatively, the effect on the threshold applied on $\hat{\alpha}_{BS}$ is that the slower the platform tilting is, the less it is compensated (gain nonlinearity).*

For very slow platform movements (i.e. $\dot{\alpha}_{FS} < \theta$), there is even no compensation. A similar nonlinearity applied on the gravity compensation would produce a paradoxical behaviour.

4 STABILITY ANALYSIS

Assumption 1. *As done in (Lippi and Mergner, 2017; Lippi et al., 2013; Mergner, 2010), we assume the direct measurements to be equal to the corresponding variables, i.e., $\breve{\alpha}_{BS} = \alpha_{BS}$ and $\breve{\alpha}_{BF} = \alpha_{BF}$.*

Let the input to the system be

$$u = \dot{\alpha}_{FS}, \tag{13}$$

i.e., the tilting speed of the platform. The state vector is four-dimensional and equal to

$$\mathbf{x} = \begin{bmatrix} x_1 \\ x_2 \\ x_3 \\ x_4 \end{bmatrix} = \begin{bmatrix} \alpha_{BS} \\ \dot{\alpha}_{BS} \\ \hat{\alpha}_{BS} \\ \alpha_{FS} \end{bmatrix}. \tag{14}$$

Starting from (2), we derive a model for the system at hand, by incorporating (4), (6), (8), (10), and (11). This yields the following system:

$$\begin{cases} \dot{x}_1 &= x_2 \\ \dot{x}_2 &= a_1 x_1 + a_2 x_2 + a_3 x_3 + a_4 x_4 + f(u) \\ \dot{x}_3 &= b x_1 + x_2 - b x_3 - b x_4 + g(u) \\ \dot{x}_4 &= u \end{cases} \tag{15}$$

where

$$a_1 = \frac{K_p^p + K_d^a c_L + mgh_B - K_G}{J_B}, \tag{16}$$

$$a_2 = \frac{K_d^a + K_d^p}{J_B}, \tag{17}$$

$$a_3 = \frac{K_p^a - c_L K_d^a}{J_B}, \tag{18}$$

$$a_4 = \frac{K_p^p - c_L K_d^a}{J_B}, \tag{19}$$

$$b = C_L, \tag{20}$$

$$g(u) = \rho(u) - u, \tag{21}$$

$$f(u) = K_d^a g(u) - K_d^p u. \tag{22}$$

Note that the nonlinearity brought about by $\rho(\cdot)$ affects the system only through input u. Figure 3 illustrates $f(u)$ and $g(u)$.

System (15) can be also written in matrix form[1], i.e.,

$$\dot{\mathbf{x}}(t) = A\mathbf{x}(t) + B(u(t)), \tag{23}$$

[1] In this case we explicitly report the dependence on time.

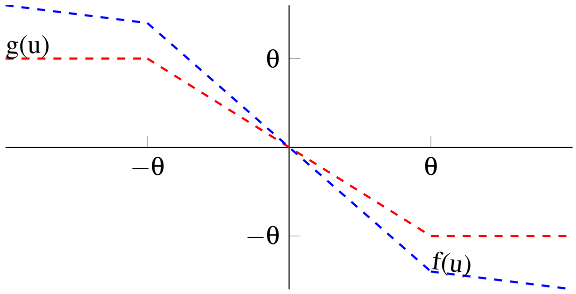

Figure 3: $f(u)$ and $g(u)$.

where

$$A := \begin{bmatrix} 0 & 1 & 0 & 0 \\ a_1 & a_2 & a_3 & a_4 \\ b & 1 & -b & -b \\ 0 & 0 & 0 & 0 \end{bmatrix} \tag{24}$$

and

$$B(u) := \begin{bmatrix} 0 \\ f(u(t)) \\ g(u(t)) \\ u(t) \end{bmatrix}. \tag{25}$$

System (23) is a linear system, with nonlinearity on the control input. The dynamics of the fourth state is a simple integrator of input u, thus 0 is an eigenvalue of the system's dynamics. The remaining three eigenvalues can be determined by the choice of K_a^p and K_a^d, our design parameters. In the following the stability conditions are derived in an analytical way while in previous work the stability of the DEC was demonstrated empirically with simulations (Lippi et al., 2013) and robot experiments (Hettich et al., 2014; Ott et al., 2016; Zebenay et al., 2015).

Lemma 1. *If K_p^a and K_d^a are chosen such that*

$$K_d^a < c_L J_B - K_d^p, \tag{26}$$

$$K_p^a + K_d^a c_L < K_G - mgh_B - K_p^p - c_L k_d^p, \tag{27}$$

$$K_p^a < K_G - mgh_B - K_p^p, \tag{28}$$

then system (23) has three eigenvalue with negative real part.

Proof. By definition of eigenvalues, the spectrum of A is

$$\mathrm{eig}(A) = \{0\} \cup \mathrm{eig}(\tilde{A}),$$

where

$$\tilde{A} := \begin{bmatrix} 0 & 1 & 0 \\ a_1 & a_2 & a_3 \\ b & 1 & -b \end{bmatrix}.$$

The characteristic polynomial of $\tilde{A}$, whose solutions are $\tilde{A}$'s eigenvalues, is:

$$p_A(\lambda) = \lambda^3 + (b - a_2)\lambda^2 + (-a_3 - a_2 b - a_1)\lambda - b(a_1 + a_3).$$

By the Descartes *Rule of Signs*, we can impose that all eigenvalues of $\tilde{A}$ have negative real part, by holding

$$\begin{cases} b - a_2 > 0 \\ -a_3 - a_2 b - a_1 > 0 \\ -b(a_1 + a_3) > 0 \end{cases} .$$

This latter becomes a set of inequalities in K_d^a and K_p^a, by incorporating (16)-(20). This yields (26)-(28), thus concluding the proof. □

Lemma 2. *The solution to system (23) is*

$$\mathbf{x}(t) = e^{At}\mathbf{x}(0) + \int_0^t e^{A(t-\tau)} B(u(\tau)) d\tau. \tag{29}$$

Proof. Let $u_1(t) := f(u(t))$, $u_2(t) := g(u(t))$, and $u_3(t) := u(t)$. We have

$$\dot{\mathbf{x}}(t) = A\mathbf{x}(t) + \tilde{B}\tilde{\mathbf{u}}(t), \tag{30}$$

with

$$\tilde{B}\tilde{\mathbf{u}}(t) = B(u(t)) \tag{31}$$

where $\tilde{\mathbf{u}}(t) := [u_1(t), u_2(t), u_3(t)]'$ and

$$\tilde{B} := \begin{bmatrix} 0 & 0 & 0 \\ 1 & 0 & 0 \\ 0 & 1 & 0 \\ 0 & 0 & 1 \end{bmatrix}.$$

By (Skogestad and Postlethwaite, 2007, (4.7)),

$$\mathbf{x}(t) = e^{At}\mathbf{x}(0) + \int_0^t e^{A(t-\tau)} \tilde{B}\tilde{\mathbf{u}}(\tau) d\tau,$$

which, by incorporating (31), yields (29), thus concluding the proof. □

In (29), the first addendum is the free response, and the integral is referred to as forced response. By (29), system's stability is determined only by matrix A, thus the nonlinearity acting on the input, i.e., $B(u(t))$, does not play any role for stability. The following two definitions of stability are extracted from (Mellodge, 2015, Chapter 3) and (Bernstein and Bhat, 1995).

Definition 1 (Asymptotic Stability)**.** *System (30) is asymptotically stable if and only if all the eigenvalues of A are in the left half of the complex plane.*

Definition 2 (Lyapunov Stability)**.** *System (30) is Lyapunov stable if and only if no eigenvalues of A are in the right half of the complex plane and all eigenvalues on the imaginary axis are semisimple (i.e., they have algebraic multiplicity equal to the geometric multiplicity).*

Theorem 1. *If K_p^a and K_d^a are chosen as in Lemma 1, system (23) is Lyapunov stable, but not asymptotically stable.*

Proof. Consider system (30) which is an equivalent of (23). Clearly, system (30) is Lyapunov stable (asymptotically stable) if and only if also (23) is Lyapunov stable (asymptotically stable).
By Lemma 1, matrix A has three eigenvalues with negative real part and one eigenvalue (the integrator in x_4) which is on the imaginary axis and semisimple. By Definition 2, system (30) is Lyapunov stable. By Definition 2, system (30) is not asymptotically stable, thus the proof is concluded. □

The non-linear system can be stabilised by choosing the appropriate pair of proportional and derivative coefficients for the PD controller.

5 SIMULATION

The parameters, defined on the basis of human anthropometrics (see (Winter, 2009)) and previous posture control analysis (see (Mergner et al., 2009; Mergner et al., 2003; Hettich et al., 2014)), are shown in Table 2. With the specific set of parameters, and by (26)-(28),

Table 2: System parameters.

Parameter	Value
J_B	71.55 $\mathrm{Kg} \cdot \mathrm{m}^2$
K_g	0.8
K_p^p	157.31 $N \cdot \mathrm{m}$
K_d^p	39.32 $N \cdot \mathrm{m} \cdot s$
c_L	0.0125 s^{-1}
θ	0.0028 *rad*
m	80 Kg
h	1.80 m

we design

$$K_p^a = -1200 \; N \cdot \mathrm{m}$$

and

$$K_d^a = -1000 \; N \cdot \mathrm{m} \cdot \mathrm{s}.$$

The behavior of the system is shown in regime of free response with no support surface tilt velocity, and forced response with a periodic input. Specifically the following conditions are simulated:

Condition 1: free response with

$$\mathbf{x}(0) = [\pi/10, 0.1, \pi/10, 0]^T.$$

The free response with no support surface tilt is the characteristic one of a linear second-order system (see Fig. 4). This happens because the nonlinearity affects only the input $u(t)$. The leaky integrator used in the

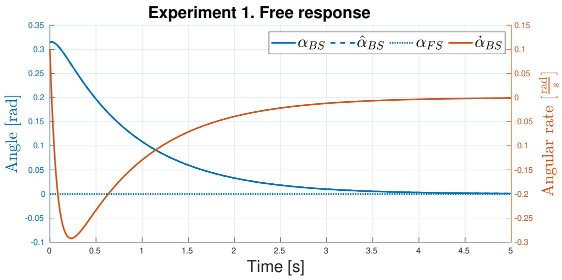

Figure 4: Free response with horizontal support surface and initial conditions $\mathbf{x}(0) = [\pi/10, 0.1, \pi/10, 0]^T$. The estimate $\hat{\alpha}_{BS}$ is equivalent to α_{BS} when $\alpha_{FS} = 0$.

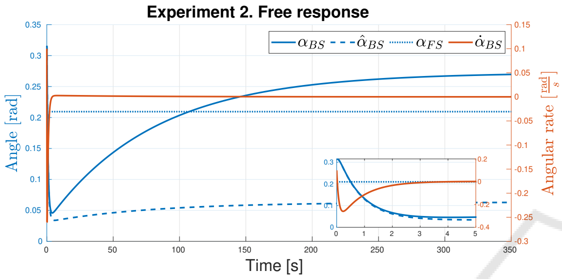

Figure 5: Free response with tilted, but not moving, support surface and non-zero initial body sway velocity and body lean, i.e. $\mathbf{x}(0) = [\pi/10, 0.1, \pi/10, \pi/15]^T$. The smaller plot shows the transient during the first 5 seconds.

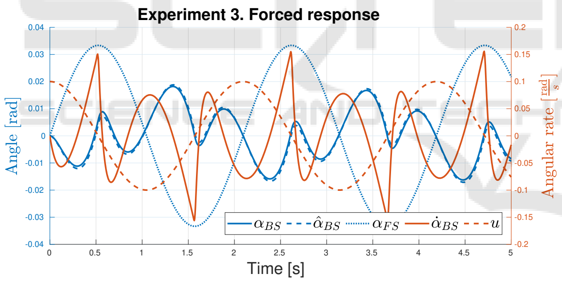

Figure 6: Forced response to sinusoidal support tilt with initial conditions $\mathbf{x}(0) = [0, 0, 0, 0]^T$, and input $u(t) = 0.1\cos(10t)$.

estimate of α_{FS} is constantly at zero.

Condition 2: free response with

$$\mathbf{x}(0) = [\pi/10, 0.1, \pi/10, \pi/15]^T.$$

The free response with a constant support surface tilt is shown in Fig. 5. The response is again the characteristic of a linear system, in which x_4 behaves as a constant signal affecting the dynamics of x_2 and x_3. There is a residual lean α_{BS} due to the error in body sway estimate $\hat{\alpha}_{BS}$.

Condition 3: forced response with

$$\mathbf{x}(0) = [0, 0, 0, 0]^T$$

and

$$u(t) = 0.1\cos(10t).$$

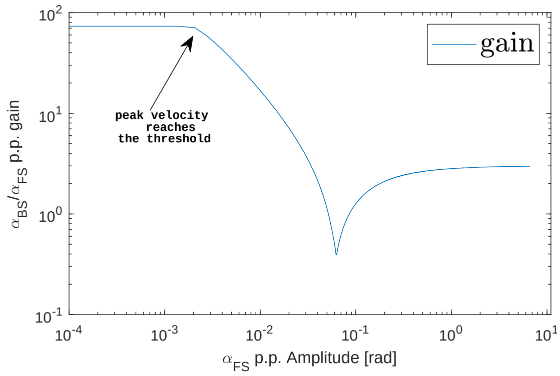

Figure 7: Support surface tilt to body sway gain with sinusoidal support tilt at different amplitude. The gain is computed as the ratio between peak to peak amplitude for of the input and the one of the output. Smaller support surface tilt are associated with larger gains because they are under-compensated due to the nonlinearity. The plateau on the left is the zone of linear behavior that happens when the support surface rotation speed is always under threshold θ. For larger amplitudes the gain tends asymptotically to a constant gain, i.e. linear behavior.

The forced response shows a partial rejection of the external disturbance. The effect of the nonlinearity is reflected in the difference between α_{BS} and its estimated value $\hat{\alpha}_{BS}$. The simulations is repeated with different amplitudes for the support surface tilt profile, producing the results in Fig. 7. The gain, in this context defined as the ratio between peak to peak amplitude for of the input and the output is plotted for different amplitudes. Smaller support surface tilt are associated with larger gains because they are under-compensated due to the nonlinearity. Specifically the plateau on the left is the zone of linear behavior that happens when the support surface rotation speed is always under threshold θ and the disturbance is not compensated. For larger amplitudes the gain tends asymptotically to a constant gain because the signal is almost always above the threshold.

6 CONCLUSIONS AND FUTURE WORK

The formal analysis of the system has provided a condition for the stability, specifically on the gains of the PD controller, i.e., (26)-(28). This confirms the idea, suggested by empirical experiments with human subjects and robots, that the nonlinearity is *benign* in that it does not endanger the stability of the system. There is the hypothesis that such dead-band nonlinearity could be useful in cutting out vestibular noise, especially when the support surface is not moving (that is the most common scenario in nature). In order to study the effect of the threshold on noise future work may integrate methods for the analysis of stochastic systems (Han. et al., 2018; Björnsson. et al., 2018). Another important aspect in posture control, that was not considered here, is the effect of delay. Delay imposes a limitation on feedback gain that can be considered the motivation for the feed-forward compensation of external disturbances (in this work, gravity). The effects of delay have been studied formally in the linear case (Antritter et al., 2014), but not yet with the nonlinear system. As the DEC has also been applied to multiple degrees of freedom scenarios (Lippi et al., 2019b; Lippi and Mergner, 2017) the formal study may be extended to multiple inverted pendulum models. A way to tackle the complexity of the multiple DoF problem may require the use of numerical methods for the study of the stability (Giesl. et al., 2018; Björnsson. and Hafstein., 2018; Giesl. and Mohammed., 2018), this will require a particular effort considering the number of state variables required to represent the dynamics of the mechanical degrees of freedom, the dynamics of the sensory estimates (e.g. the leaky integrator in the presented work) and the ones used to represent the delays.

ACKNOWLEDGEMENTS

This work is supported by the project COMTEST (Lippi et al., 2019a), a sub-project of EUROBENCH (European Robotic Framework for Bipedal Locomotion Benchmarking, www.eurobench2020.eu) funded by H2020 Topic ICT 27-2017 under grant agreement number 779963.

REFERENCES

Abedi, P. and Shoushtari, A. L. (2012). Modelling and simulation of human-like movements for humanoid robots. In *Proceedings of the 9th International Conference on Informatics in Control, Automation and Robotics - Volume 1: ICINCO*, pages 342–346. INSTICC, SciTePress.

Alexandrov, A. V., Lippi, V., Mergner, T., Frolov, A. A., Hettich, G., and Husek, D. (2017). Human-inspired eigenmovement concept provides coupling-free sensorimotor control in humanoid robot. *Frontiers in neurorobotics*, 11:22.

Antritter, F., Scholz, F., Hettich, G., and Mergner, T. (2014). Stability analysis of human stance control from the system theoretic point of view. In *Control Conference (ECC), 2014 European*, pages 1849–1855. IEEE.

Atkeson, C. G. and Stephens, B. (2007). Multiple balance strategies from one optimization criterion. In *2007 7th IEEE-RAS International Conference on Humanoid Robots*, pages 57–64. IEEE.

Bernstein, D. S. and Bhat, S. P. (1995). Lyapunov stability, semistability, and asymptotic stability of matrix second-order systems. *Journal of mechanical design*, 117(B):145–153.

Björnsson., H., Giesl., P., Gudmundsson., S., and Hafstein., S. (2018). Local lyapunov functions for nonlinear stochastic differential equations by linearization. In *Proceedings of the 15th International Conference on Informatics in Control, Automation and Robotics - Volume 2: CTDE*, pages 579–586. INSTICC, SciTePress.

Björnsson., H. and Hafstein., S. (2018). Verification of a numerical solution to a collocation problem. In *Proceedings of the 15th International Conference on Informatics in Control, Automation and Robotics - Volume 2: CTDE*, pages 587–594. INSTICC, SciTePress.

Bleisteiner, G. and Mangoldt, W. (2013). *Handbuch der Regelungstechnik*. Springer-Verlag.

Boonstra, T. A., van Vugt, J. P., van der Kooij, H., and Bloem, B. R. (2014). Balance asymmetry in parkinson's disease and its contribution to freezing of gait. *PLoS One*, 9(7):e102493.

Engelhart, D., Boonstra, T. A., Aarts, R. G., Schouten, A. C., and van der Kooij, H. (2016). Comparison of closed-loop system identification techniques to quantify multi-joint human balance control. *Annual Reviews in Control*, 41:58–70.

Engelhart, D., Pasma, J. H., Schouten, A. C., Meskers, C. G., Maier, A. B., Mergner, T., and van der Kooij, H. (2014). Impaired standing balance in elderly: a new engineering method helps to unravel causes and effects. *Journal of the American Medical Directors Association*, 15(3):227–e1.

Giesl., P., Argáez., C., Hafstein., S., and Wendland., H. (2018). Construction of a complete lyapunov function using quadratic programming. In *Proceedings of the 15th International Conference on Informatics in Control, Automation and Robotics - Volume 2: CTDE*, pages 560–568. INSTICC, SciTePress.

Giesl., P. and Mohammed., N. (2018). Combination of refinement and verification for the construction of lyapunov functions using radial basis functions. In *Proceedings of the 15th International Conference on Informatics in Control, Automation and Robotics - Volume 2: CTDE*, pages 569–578. INSTICC, SciTePress.

Goodworth, A. D. and Peterka, R. J. (2010). Influence of stance width on frontal plane postural dynamics and coordination in human balance control. *Journal of Neurophysiology*, 104(2):1103–1118.

Goodworth, A. D. and Peterka, R. J. (2018). Identifying mechanisms of stance control: a single stimulus multiple output model-fit approach. *Journal of Neuroscience Methods*, 296:44–56.

Han., H., Hamasaki., D., and Fu., J. (2018). State- and uncertainty-observers-based controller for a class of t-s fuzzy models. In *Proceedings of the 15th International Conference on Informatics in Control, Automation and Robotics - Volume 2: CTDE*, pages 551–559. INSTICC, SciTePress.

Hettich, G., Assländer, L., Gollhofer, A., and Mergner, T. (2014). Human hip—ankle coordination emerging from multisensory feedback control. *Human Movement Science*, 37:123–146.

Hettich, G., Lippi, V., and Mergner, T. (2013). Human-like sensor fusion mechanisms in a postural control robot. In Londral, A. E., Encarnacao, P., and Pons, J. L., editors, *Proceedings of the International Congress on Neurotechnology, Electronics and Informatics. Vilamoura, Portugal*, pages 152–160.

Hettich, G., Lippi, V., and Mergner, T. (2015). Human-like sensor fusion implemented in the posture control of a bipedal robot. In *Neurotechnology, Electronics, and Informatics*, pages 29–45. Springer.

Jafari, H., Nikolakopoulos, G., and Gustafsson, T. (2019). Stabilization of an inverted pendulum via human brain inspired controller design. In *IEEE-RAS International Conference on Humanoid Robots*. IEEE.

Jeka, J. J., Allison, L. K., and Kiemel, T. (2010). The dynamics of visual reweighting in healthy and fall-prone older adults. *Journal of motor behavior*, 42(4):197–208.

Lippi, V. and Mergner, T. (2017). Human-derived disturbance estimation and compensation (dec) method lends itself to a modular sensorimotor control in a humanoid robot. *Frontiers in neurorobotics*, 11:49.

Lippi, V., Mergner, T., and Hettich, G. (2013). A bio-inspired modular system for humanoid posture control. *In: Ugur, E., Oztop, E., Morimoto, J., and Ishii, S. (Eds) Proceedings of IROS 2013 Workshop on Neuroscience and Robotics "Towards a robot-enabled, neuroscience-guided healthy society"*.

Lippi, V., Mergner, T., Seel, T., and Maurer, C. (2019a). COMTEST project: A complete modular test stand for human and humanoid posture control and balance. In *2019 IEEE-RAS 19th International Conference on Humanoid Robots (Humanoids) Toronto, Canada. October 15-17*.

Lippi, V., Mergner, T., Szumowski, M., Zurawska, M. S., and Zielińska, T. (2016). Human-inspired humanoid balancing and posture control in frontal plane. In *ROMANSY 21-Robot Design, Dynamics and Control: Proceedings of the 21st CISM-IFToMM Symposium, June 20-23, Udine, Italy*, volume 569, pages 285–292. Springer.

Lippi, V., Molinari, F., and Seel, T. (2019b). Distributed bio-inspired humanoid posture control. In *2019 41st Annual International Conference of the IEEE Engineering in Medicine and Biology Society (EMBC)*, pages 5360–5365. IEEE.

Luecke, R. H. and McGuire, M. (1968). Analysis of optimal composite feedback-feedforward control. *AIChE Journal*, 14(1):181–189.

Mellodge, P. (2015). *A Practical Approach to Dynamical Systems for Engineers*. Woodhead Publishing.

Mergner, T. (2010). A neurological view on reactive human stance control. *Annual Reviews in Control*, 34(2):77–198.

Mergner, T., Maurer, C., and Peterka, R. J. (2003). A multisensory posture control model of human upright stance. *Progress in Brain Research*, 142:189–201.

Mergner, T., Schweigart, G., and Fennell, L. (2009). Vestibular humanoid postural control. *Journal of Physiology - Paris*, 103:178–194.

Merton, P. (1953). Speculations on the servo-control of movement. In *Ciba Foundation Symposium-The Spinal Cord*, pages 247–260. Wiley Online Library.

Ott, C., Henze, B., Hettich, G., Seyde, T. N., Roa, M. A., Lippi, V., and Mergner, T. (2016). Good posture, good balance: comparison of bioinspired and model-based approaches for posture control of humanoid robots. *IEEE Robotics & Automation Magazine*, 23(1):22–33.

Pasma, J., Engelhart, D., Schouten, A., Van der Kooij, H., Maier, A., and Meskers, C. (2014). Impaired standing balance: the clinical need for closing the loop. *Neuroscience*, 267:157–165.

Peterka, R. (2002). Sensorimotor integration in human postural control. *Journal of neurophysiology*, 88(3):1097–1118.

Roffel, B. and Betlem, B. (2007). *Process dynamics and control: modeling for control and prediction*. John Wiley & Sons.

Skogestad, S. and Postlethwaite, I. (2007). *Multivariable feedback control: analysis and design*, volume 2. Wiley New York.

van Asseldonk, E. H., Buurke, J. H., Bloem, B. R., Renzenbrink, G. J., Nene, A. V., van der Helm, F. C., and van der Kooij, H. (2006). Disentangling the contribution of the paretic and non-paretic ankle to balance control in stroke patients. *Experimental neurology*, 201(2):441–451.

van der Kooij, H., van Asseldonk, E., and van der Helm, F. C. (2005). Comparison of different methods to identify and quantify balance control. *Journal of neuroscience methods*, 145(1-2):175–203.

van der Kooij, H., van Asseldonk, E. H. F., Geelen, J., van Vugt, J. P. P., and Bloem, B. R. (2007). Detecting asymmetries in balance control with system identification: first experimental results from parkinson patients. *Journal of Neural Transmission*, 114(10):1333.

Winter, D. A. (2009). *Biomechanics and motor control of human movement*. John Wiley & Sons.

Zebenay, M., Lippi, V., and Mergener, T. (2015). Human-like humanoid robot posture control. In *2015 12th International Conference on Informatics in Control, Automation and Robotics (ICINCO)*, volume 2, pages 304–309. INSTICC, SciTePress.

Zhong, H., Pao, L., and de Callafon, R. (2012). Feedforward control for disturbance rejection: Model matching and other methods. In *2012 24th Chinese Control and Decision Conference (CCDC)*, pages 3528–3533. IEEE.